An in Situ Energy-Dispersive X-ray Diffraction Study of the Hydrothermal Crystallizations of Open-Framework Gallium Oxyfluorophosphates with the ULM-3 and ULM-4 Structures

Richard I. Walton,[†] Thierry Loiseau,[‡] Dermot O'Hare,*[,†] and Gérard Férey[‡]

Inorganic Chemistry Laboratory, University of Oxford, South Parks Road, Oxford, OX1 3QR, United Kingdom, and Institut Lavoisier, UMR CNRS 8637, Université de Versailles Saint Quentin-en-Yvelines, 45 avenue des Etats-Unis, 78035 Versailles Cedex, France

Received May 5, 1999. Revised Manuscript Received September 8, 1999

The hydrothermal crystallizations of open-framework gallium oxyfluorophosphates with the ULM-3 and ULM-4 structures have been studied in situ using energy-dispersive X-ray diffraction. Data collected during reactions in a large volume (∼25 mL) cell under real laboratory conditions have allowed the growth of crystalline phosphates from amorphous gel precursors to be observed. A number of amines have been used in the syntheses, and the nature of the phosphorus source has been investigated. Kinetic data have been determined by monitoring changes in the integrated intensities of Bragg reflections and modeled using the Avrami−Erofeev expression. The results suggest that the reactions are diffusion controlled; Avrami exponents of ∼0.5 are found, and the rate of crystallization is not affected by temperature (140−200 °C). Subsequent modeling using the Jander expression confirms the diffusion-controlled nature of reaction. When P_2O_5 is used instead of the usual H_3PO_4 in the synthesis of gallium ULM-3 with 1,3-diaminopropane, a previously unknown crystalline phase is observed to form before the onset of crystallization of the product. This phase is transient and its growth and decay have a marked affect on the growth curve of the ULM-3. Attempts to recover the new phase by quenching the hydrothermal processes revealed that the intermediate gallium phase converts to a different phase on cooling, and this second novel compound was subsequently prepared at room temperature. Analytical electron microscopy shows the new material to be a gallium phosphate with Ga:P ratio of 1:2.

Introduction

The preparation of new microporous materials with chemical and physical properties suited for a particular application often involves a "trial and error" approach, whereby a large number of reaction parameters must be varied. Open-framework inorganic solids are commonly prepared using a solvothermal method, whereby solid and liquid reagents are combined with a solvent (usually water and hence hydrothermal conditions) and heated in sealed vessel. It would be very desirable if the product of a hydrothermal reaction could be predicted, and a material "tailor-made" by choice of starting materials and reaction conditions. The choice of temperature, reaction time, reagents and solvent, percentage fill of vessel, and many other factors can influence the outcome of a reaction, but the interplay of these parameters is poorly understood. A number of possible reaction mechanisms have been postulated for the formation of some families of microporous solids,[1,2] and computer modeling used to help predict the outcome of certain hydrothermal reactions,[3,4] but few experimental data are available to enable a full understanding of the processes involved in the hydrothermal formation of a complex inorganic solid.

The study of hydrothermal reactions in situ, using a noninvasive probe to follow changes of a certain chemical or physical property under real laboratory conditions, has begun provide the first information toward formulating reaction mechanisms.[5,6] In situ X-ray diffraction is an especially powerful technique since it allows the formation of crystalline phases to be monitored quantitatively as reactions occur. A number of workers have previously concentrated on the study of the formation of transition metal aluminum phosphates, using both angular[7−11] and energy-dispersive X-ray

* Author for correspondence: email dermot.ohare@chem.ox.ac.uk.
[†] University of Oxford.
[‡] Université de Versailles.

(1) Ferey, G. *J. Fluorine Chem.* **1995**, *72*, 187.
(2) Oliver, S.; Kuperman, A.; Ozin, G. A. *Angew. Chem., Int. Ed. Engl.* **1998**, *37*, 46.
(3) Lewis, D. W.; Catlow, C. R. A.; Thomas, J. M. *Faraday Discuss.* **1997**, *106*, 451.
(4) Lewis, D. W.; Sankar, G.; Wyles, J. K.; Thomas, J. M.; Catlow, C. R. A.; Willcock, D. J. *Angew. Chem., Int. Ed. Engl.* **1997**, *36*, 2675.
(5) Cheetham, A. K.; Mellot, C. F. *Chem. Mater.* **1997**, *9*, 2269.
(6) Francis, R. J.; O'Hare, D. *J. Chem. Soc., Dalton Trans.* **1998**, 3133.
(7) Norby, P.; Christensen, A. N.; Hanson, J. C. *Stud. Surf. Sci. Catal.* **1994**, *84*, 179.
(8) Christensen, A. N.; Norby, P.; Hanson, J. C. *Acta Chem. Scand.* **1997**, *51*, 249.

10.1021/cm990271c CCC: $18.00
Published on Web 10/28/1999

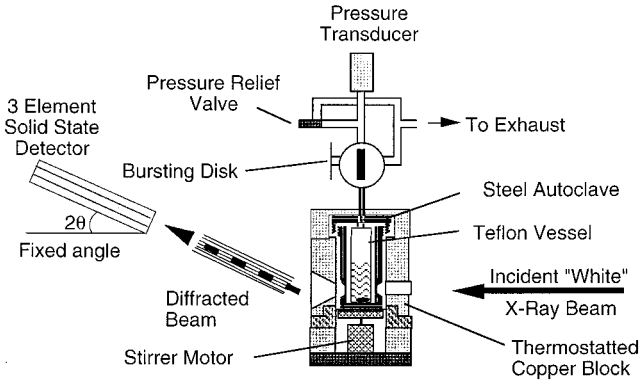

Figure 1. A schematic of the in situ energy-dispersive X-ray diffraction hydrothermal apparatus used on Station 16.4 of the Daresbury SRS.

diffraction.[12−14] Energy-dispersive X-ray diffraction (EDXRD) using synchrotron-generated white-beam radiation allows the use of bulky reaction vessels, whereas angular-dispersive diffraction requires a monochromatic X-ray beam and a small sample volume and thin-walled reaction vessels must be used.[15] In previous work, our group in Oxford and workers at the U.K. synchrotron radiation source at Daresbury Laboratory have used the EDXRD technique to study hydrothermal reactions in situ.[16−18] Our apparatus, Figure 1, has the advantage over other methods available, in particular those using small reaction vessels, in that reactions are studied under real conditions since the reaction cell is a laboratory-sized vessel, which is only slightly modified to allow diffraction data to be collected.

Open-framework phosphates, which are the subject of this paper, have been widely studied since the discovery of aluminum phosphates with zeolite-like structures, in the early 1980s.[19,20] Research into the synthesis of the phosphates has been driven by their potential application in areas which zeolites have long found use: shape-selective catalysis, molecular sieving, and gas absorption, for example.[21,22] The phosphates have provided new microporous frameworks, since the constituent metal polyhedra are not limited to tetrahedra like the aluminosilicate zeolites, and it has become apparent that a large number of elements, including transition metals and main group metals, readily form open phosphates frameworks, or can be incorporated into those of Group 13 metals.[23] Although the phosphates suffer from poor thermal stability compared to the aluminosilicate zeolites, and often as-prepared are not strictly microporous since they contain charge-balancing organic species, the novel structure types, and the potential for tunable properties by incorporation of transition metals into a framework structure, have maintained interest in these compounds. Indeed in certain cases potential applications mentioned above for open-framework phosphates have been realized, for example, SAPO-11 is used industrially as a support for a platinum lube−dewaxing catalyst,[24] and recently Thomas et al. have shown that transition metal substituted aluminophosphates catalyze the oxidation of alkanes.[25] We have chosen the ULM-*n* family of gallium and aluminum phosphates as a model system to investigate the mechanism of crystallization of metal phosphates. The ULM-*n* compounds have closely related structures which have been well-characterized using a number of methods.[1,26] Most importantly for in situ studies, the majority of the compounds may be prepared pure as polycrystalline powders. We have recently used the EDXRD apparatus to study the formation of the large-pore gallium oxyfluorophosphate ULM-5, and for the first time observed transient intermediate crystalline phases during the hydrothermal preparation of a phosphate, as well as extracting high-quality kinetic data.[27,28] We intend using a number of in situ methods to follow the hydrothermal syntheses of the ULM-*n* compounds; recently, some of us have described an in situ NMR spectroscopic study of related reactions.[29] In this paper we describe our in situ EDXRD study of the crystallization of gallium oxyfluorophosphates with the ULM-3[30] and ULM-4[31] structures. These two framework structures, both with composition $M_3P_3O_{12}F_2^{2-}$, are closely related and may be thought of as being made up of the same hexameric "secondary building unit" (Figure 2). Both are three-dimensional frameworks containing channels in which charge-balancing alkylammonium cations reside, and in the case of ULM-3 also occluded water molecules. Pure gallium oxyfluorophosphates may be prepared with both structure types using a number of amines as structure directing agents and in one case, 1,3-diaminopropane, either framework may be synthesized pure by altering the initial gel pH.[32]

(9) Christensen, A. N.; Jensen, T. R.; Norby, P.; Hanson, J. C. *Chem. Mater.* **1998**, *10*, 1688.
(10) Norby, P.; Hanson, J. C. *Catal. Today* **1998**, *39*, 301.
(11) Norby, P.; Christensen, A. N.; Hanson, J. C. *Inorg. Chem.* **1999**, *38*, 1216.
(12) Rey, F.; Sankar, G.; Thomas, J. M.; Barrett, P. A.; Lewis, D. W.; Catlow, C. R. A.; Clark, S. M.; Greaves, G. N. *Chem. Mater.* **1995**, *7*, 1435.
(13) Rey, F.; Sankar, G.; Thomas, J. M.; Barrett, P. A.; Lewis, D. W.; Catlow, C. R. A.; Clark, S. M.; Greaves, G. N. *Chem. Mater.* **1996**, *8*, 590.
(14) Davies, A. T.; Sankar, G.; Catlow, C. R. A.; Clark, S. M. *J. Phys. Chem. B* **1997**, *101*, 10115.
(15) Munn, J.; Barnes, P.; Hausermann, D.; Axon, S. A.; Klinowski, J. *Phase Transitions* **1992**, *39*, 129.
(16) Evans, J. S. O.; Francis, R. J.; O'Hare, D.; Price, S. J.; Clarke, S. M.; Flaherty, J.; Gordon, J.; Nield, A.; Tang, C. C. *Rev. Sci. Instrum.* **1995**, *66*, 2442.
(17) Clark, S. M.; Nield, A.; Rathbone, T.; Flaherty, J.; Tang, C. C.; Evans, J. S. O.; Francis, R. J.; O'Hare, D. *Nucl. Instrum. Methods B* **1995**, *97*, 98.
(18) Francis, R. J.; Price, S. J.; Evans, J. S. O.; O'Brien, S.; O'Hare, D.; Clark, S. M. *Chem. Mater.* **1996**, *8*, 2102.
(19) Wilson, S. T.; Lok, B. M.; Messina, C. A.; Cannan, T. R.; Flanigen, E. M. *J. Am. Chem. Soc.* **1982**, *104*, 1146.
(20) Wilson, S. T.; Lok, B. M.; Messina, C. A.; Cannon, T. R.; Flanigen, E. M. *ACS Symp. Ser.* **1983**, *218*, 79.
(21) Haag, W. O. *Zeolites and Related Microporous Materials: State of the Art* **1994**, *84B*, 1375.
(22) Zones, S. I.; Davis, M. E. *Curr. Opin. Solid State Mater. Chem.* **1996**, *1*, 107.
(23) Weller, M. T.; Dann, S. E. *Curr. Opin. Solid State Mater. Sci.* **1998**, *3*, 137.
(24) Miller, S. *Microporous Mater.* **1994**, *2*, 439.
(25) Thomas, J. M.; Raja, R.; Sankar, G.; Bell, R. *Nature* **1999**, *398*, 226.
(26) Ferey, G. *C. R. Acad. Sci. Paris Ser. IIc* **1998**, *1*, 1−13.
(27) Francis, R. J.; Price, S. J.; O'Brien, S.; Fogg, A. M.; O'Hare, D.; Loiseau, T.; Ferey, G. *Chem. Commun.* **1997**, 521.
(28) Francis, R. J.; O'Brien, S.; Fogg, A. M.; Halasyamani, P. S.; O'Hare, D.; Loiseau, T.; Ferey, G. *J. Am. Chem. Soc.* **1999**, *121*, 1002.
(29) Haouas, M.; Gerardin, C.; Taulelle, F.; Estournes, C.; Loiseau, T.; Ferey, G. *J. Chim. Phys.* **1997**, *95*, 302.
(30) Loiseau, T.; Retoux, R.; Lacorre, P.; Ferey, G. *J. Solid State Chem.* **1994**, *111*, 427.
(31) Cavellec, M.; Riou, D.; Ferey, G. *Eur. J. Solid State Inorg. Chem.* **1994**, *31*, 583.
(32) Loiseau, T.; Taulelle, F.; Ferey, G. *Microporous Mater.* **1996**, *5*, 365.

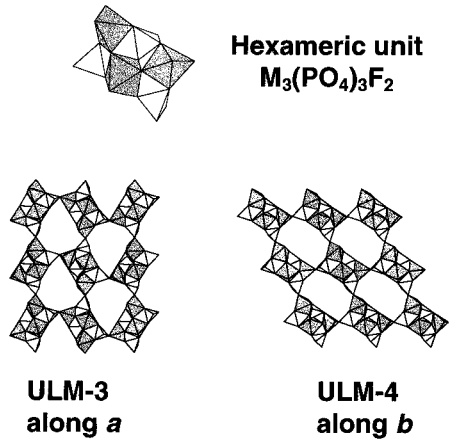

Figure 2. Representations of the anionic frameworks of ULM-3 and ULM-4 showing how they may be considered as being constructed from the same hexameric "secondary building unit".

Table 1. Gel Compositions Used To Prepare Gallium Oxyfluorophosphates with the ULM-3 and ULM-4 Structures[a]

compound	amine (A)	gel composition
ULM-3 (Ga)	1,3-diamino-propane	Ga_2O_3:1.0 P_2O_5:2.0 HF:1.9 A:70 H_2O
ULM-3 (Ga)	1,4-diamino-butane	Ga_2O_3:1.0 P_2O_5:2.0 HF:1.9 A:70 H_2O
ULM-4 (Ga)	methylamine	Ga_2O_3:1.0 P_2O_5:1.0 HF:A:40 H_2O
ULM-4 (Ga)	1,3-diamino-propane	Ga_2O_3:1.5 P_2O_5:2.0 HF:0.8 A:70 H_2O

[a] As is conventional in molecular sieve chemistry, the relative amounts of metal and phosphorus source are expressed in terms of their respective oxide.

Experimental Section

Materials. All chemicals were purchased from chemical companies and used as supplied: Ga_2O_3 (Aldrich 99.99%), orthophosphoric acid, H_3PO_4, (BDH, 85% in water), P_2O_5 (BDH), hydrofluoric acid (Fisons, 40% in water), 1,3-diaminopropane, $NH_2(CH_2)_3NH_2$ (Aldrich 99%), 1,4-diaminobutane, $NH_2(CH_2)_4NH_2$ (Aldrich 99%), methylamine, CH_3NH_2 (Aldrich 40% in water). An X-ray powder diffraction pattern of "Ga_2O_3" showed it to consist of poorly crystalline β-Ga_2O_3 and crystalline GaOOH (disapore structure type).

The in Situ EDXRD Experiment. Energy-dispersive X-ray diffraction experiments were performed on Station 16.4 of the Daresbury SRS using apparatus previously described.[16] The synchrotron source operates with an average stored current of 200 mA and a typical beam energy of 2 GeV. Station 16.4 is illuminated with radiation from a 6 T superconducting wiggler and receives X-rays over a energy range 5−120 keV with a maximum X-ray flux of 3×10^{10} photons/s at around 13 keV. The position of this energy maximum is shifted by the absorption of lower energy photons by the apparatus so that in practice X-rays with energies above ∼30 keV are useful. Briefly, the hydrothermal cell is a similar volume to those available commercially for laboratory use (∼25 mL), but a has thinner stainless steel outer case (0.4 mm) to minimize absorption of X-rays. A series of experiments was performed on ULM-3 and ULM-4 syntheses, using a number of different amines, phosphorus sources, and temperatures; gel compositions are summarized in Table 1. In each reaction performed, ∼1 g of metal source was dispersed in ∼10 cm^3 of distilled water by stirring with use of a magnetic flea. The phosphorus source, hydrofluoric acid, and finally the amine were added, the mixture stirred for a few moments and then was sealed in the cell and transferred to the preheated apparatus. The time between mixing reagents and beginning data collection was always less than 5 min and although introducing the cold cell causes cooling of the heating block, constant desired temperature was attained in ∼5 min. The reaction mixture was stirred continually during data collection to ensure solid material remained in the beam at all times and did not settle out. X-ray diffraction patterns were recorded every 30 s by a three-element solid-state detector, recently described by Colston et al.[33] Each detector element is separated by an angle of ∼3° so that a d spacing range of greater than 20 Å may be observed in a given experiment. In the current work the lower detector was always set at $2\theta \approx 2.0°$, so that the strong high d spacing Bragg reflections of the ULM-3 and ULM-4 materials (at 9.20 and 8.71 Å respectively) appeared in the region of the optimum energy position of the energy-dispersive spectrum. For the energy-dispersive diffraction experiment, E (keV) = 6.19926/(d sin θ) for a Bragg refection arising from a plane of d (in angstroms). A pre-prepared sample of gallium ULM-3 was stirred in 10 cm^3 of water within the hydrothermal cell and the position of the four strongest Bragg reflections used to determine accurately the angle of the detector (2θ).

Electron Microscopy. In a number of cases, samples of material recovered after quenching ULM-n syntheses were analyzed by electron microscopy. A JEOL 2000FX transmission electron microscope was used, equipped with a Link "Pentafet" EDX detector (Be window) and attached to a eXL hardware interface. A highly crystalline sample of $GaPO_4$, prepared by hydrothermal reaction between Ga_2O_3 and H_3PO_4, was studied to calculate a calibration constant to relate the relative atomic concentration of gallium and phosphorus to the observed ratios of intensities of gallium-L and phosphorus-K X-ray emissions (the ratio method).[34] Typically 15 crystallites of each sample were analyzed.

Results

Kinetic Study of the Direct Hydrothermal Crystallization of Gallium ULM-3 and ULM-4 Phosphates. Figure 3 shows plots of typical time-resolved EDXRD data during the crystallization of gallium ULM-3 and ULM-4. The detector was set at $2\theta = 2.05°$. For gallium ULM-3 prepared using H_3PO_4, three distinct diffraction features are observed to form from the amorphous starting mixture after a short (∼10 min) time, and these correspond to the five strongest Bragg reflections of the compound [(020) at 9.20 Å, (021) at 7.94 Å, (002) at 7.89 Å, (111) at 7.74 Å, and (112) at 5.90 Å]. The inherent low-resolution of the energy-dispersive technique is apparent here, since the three closely lying (021), (002), and (111) reflections are not completely resolved, but it can be seen that each feature smoothly increases in intensity with time. The next strongest Bragg reflection of ULM-3 is expected at 5.08 Å, and this overlaps with a diffraction feature due to the Teflon liner of the cell at 4.92 Å (not shown). In the case of ULM-4 (Figure 3b), three distinct intense features are observed by the low-angle detector and these correspond to the three most intense Bragg reflections of ULM-4 [the (002) at 8.39 Å, (10$\bar{1}$) at 7.93 Å, and (110) at 6.60 Å]. As with ULM-3, these smoothly increase in intensity with time after a short induction period of ∼10 min.

Figure 4 shows the results of peak area determination using an automated Gaussian-fitting routine, for each of the data sets shown in Figure 3. These growth curves are expressed in terms of extent of reaction, scaled from

(33) Colston, S. L.; Jacques, S. D. M.; Barnes, P.; Jupe, A. C.; Hall, C. *J. Synchrotron Rad.* **1998**, *5*, 112.
(34) Cheetham, A. K.; Skarnulis, A. J. *Anal. Chem.* **1981**, *53*, 1060.

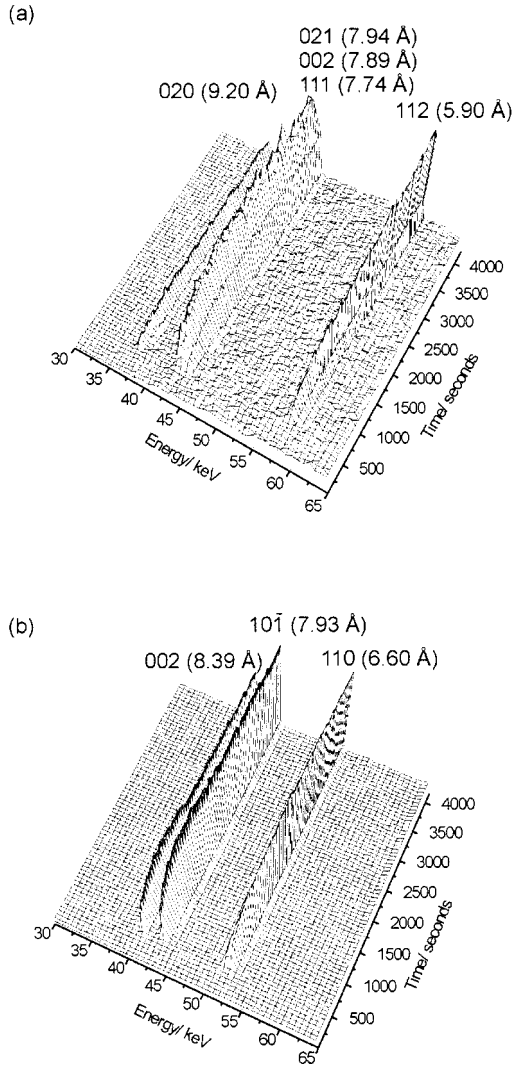

Figure 3. Three-dimensional plots of diffraction data collected during the hydrothermal crystallization of (a) gallium ULM-3 prepared using 1,3-diaminopropane and orthophosphoric acid at 180 °C and (b) gallium ULM-4 prepared using methylamine and orthophosphoric acid at 180 °C.

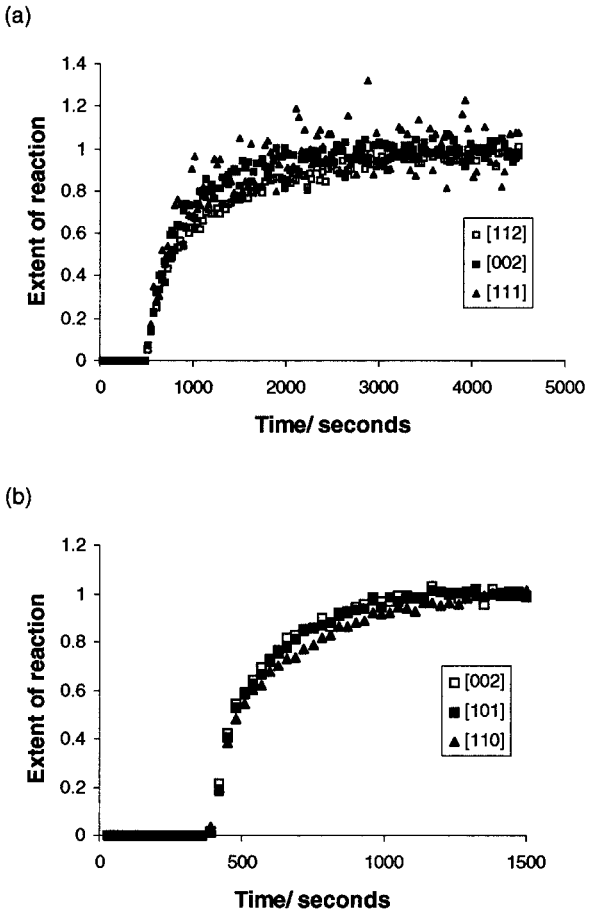

Figure 4. Crystallization curves determined by Gaussian fitting for (a) gallium ULM-3 prepared using 1,3-diaminopropane and orthophosphoric acid at 180 °C and (b) gallium ULM-4 prepared using methylamine and orthophosphoric acid at 180 °C.

zero to one and were determined by normalization to the maximum intensity of the Bragg reflection (see below). For each compound, the Bragg reflections studied appear at exactly the time and growth curves representing each peak area growth have similar shapes, suggesting that in each crystal growth is isotropic in each crystallographic direction. The growth curves highlight the extremely short induction time of the crystallizations and show that ~80% of reaction in each case is complete after less than an hour of heating. This behavior is consistent with a previous study by some of us on the crystallization of the oxyfluorogallophosphate ULM-5,[27,28] where similarly short induction times and total reaction times were observed.

Crystal growth curves such as those shown in Figure 4 are often simulated using the Avrami−Eroféev expression. This kinetic expression has been widely used in solid-state chemistry as a means of modeling, for example, phase transitions and crystal growth, and is often used to interpret the crystallization curves of zeolites.[35−38] The Avrami−Eroféev expression simply relates the extent of reaction, α, scaled from zero at the beginning of reaction and unity at the end, to the time coordinate t and may be expressed as

$$\alpha = 1 - \exp\{-(k(t - t_0))^n\} \qquad (1)$$

t_0 is the induction time of the process studied, k the rate constant, and n the Avrami exponent. The value of n contains information about the mechanism of the process studied. Hulbert analyzed various possible ideal reaction situations and tabulated expected values of n for each, taking into account a variety of factors that might influence crystal growth.[39] The interpretation of the Avrami exponent is, however, far from straightforward and often independent experimental information is required to establish a mechanism, since a given value of n does not always unequivocally allow different types of reaction mechanisms to be distinguished.

For the crystallization curves shown in Figure 4, least-squares refinement of the Avrami−Eroféev expression was performed. The extent of reaction at a given time, may be defined as the ratio of peak intensity at time that time, I_t, to maximum peak intensity, I_{max}, when crystallization is complete. This assumes that the total mass of diffracting sample remains constant.[40]

(35) Avrami, M. *J. Chem. Phys.* **1939**, *7*, 1103.
(36) Avrami, M. *J. Chem. Phys.* **1940**, *8*, 212.
(37) Avrami, M. *J. Chem. Phys.* **1941**, *9*, 177.
(38) Eroféev, B. V. *C. R. Dokl. Acad. Sci. URSS* **1946**, *52*, 511.
(39) Hulbert, S. F. *J. Br. Ceram. Soc.* **1969**, *6*, 11.

Thus the Avrami−Eroféev expression can be written as

$$I_t = I_{max}\,[1 - \exp\{-(k(t - t_0))^n\}] \qquad (2)$$

The value of I_{max} is essentially a normalization factor to account the fact that not all reactions studied here reached completion; although for each reaction studied initial product formation was rapid and ~80% of product had formed within an hour, the final stage of reaction required several hours further heating and it was often difficult to judge if the reaction had finished while data collection was taking place. t_0 was fixed at the experimentally observed value, the time taken for the Bragg reflection to appear, and I_{max}, n, and k varied in least-squares refinement. The calculated value of I_{max} was later used to normalize the data, and present kinetic curves in terms of α. Because of the possible correlation between n and k when performing least-squares refinements a better approach to data analysis is to plot ln(−ln(1 − α)) vs ln($t - t_0$) and determine n and k from the gradient and intercept. Such analysis was performed by Sharp and Hancock and is derived by taking logarithms twice of the Avrami−Eroféev expression (eq 2):[41]

$$\ln[-\ln(1 - \alpha)] = n \ln(t) - n \ln(k) \qquad (3)$$

Figure 5 shows Sharp−Hancock plots of the kinetic data extracted by the study of the two well-resolved (112) and (110) Bragg reflections of ULM-3 and ULM-4, respectively, for the two crystallizations already discussed using the calculated values of α over the range $0.1 < \alpha < 0.9$. The graphs produced are linear over the whole extent of data and the gradient and intercept of lines fitted by linear regression allow kinetic parameters to be extracted. Table 2 contains parameters obtained by analysis of data collected from gallium ULM-3 syntheses at a number of different temperatures for two different amines. In each case linear graphs were obtained for $0.1 < \alpha < 0.9$, indicating a single reaction mechanism for the largest part of crystal growth. Two features of the parameters derived are noteworthy. First that Avrami exponents of less than 1, and close to 0.5, are always produced, and second that there is no obvious dependence of rate constant of crystallization on temperature. According to Hulbert, Avrami exponents of ~0.5 are expected *uniquely* when a reaction is diffusion controlled; for all other reaction scenarios, n is expected to be 1 or greater.[39] To confirm this result, least-squares refinement of the Avrami expression to the intensity data were performed with n fixed at 1, 2, 3, and 4. In every case, a considerably poorer fit result than for the lower value of n, and if the exponent was allowed to vary from its starting point, the originally determined value was ultimately produced. The rate constants show no trend with increasing temperature and repeated experimental runs of individual experiments resulted in a spread of rate constants very similar to that observed with temperature. This is consistent with the diffusion-controlled mechanism, i.e., it is the processes occurring in solution leading to the formation of nucleation sites for crystal growth that define the reaction mechanism and once crystallization has begun the speed of nucleation does not affect the crystal growth. Crystallization is rapid and occurs at the same rate at each of the temperatures studied, within experimental error. The induction times show a tendency to increase as

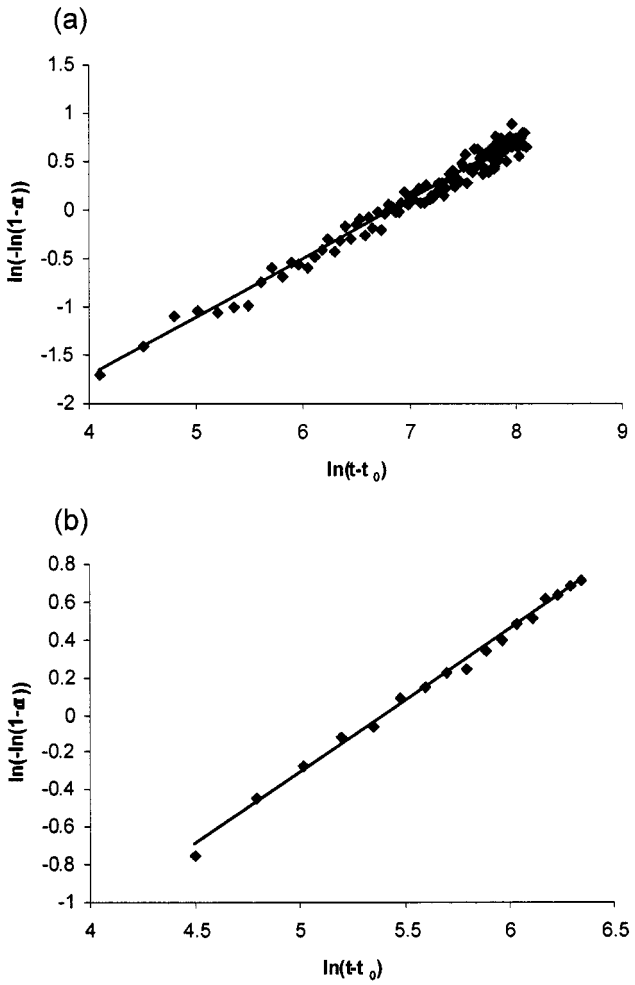

Figure 5. Sharp−Hancock plots for (a) gallium ULM-3 prepared using 1,3-diaminopropane and orthophosphoric acid at 180 °C using the growth curve derived from the (111) Bragg reflection and (b) gallium ULM-4 prepared using methylamine and orthophosphoric acid at 180 °C using the growth curve derived from the (112) Bragg reflection.

Table 2. Results of Sharp−Hancock Analysis of Kinetic Data Describing the Crystallizations of Gallium ULM-3 under Various Conditions[a]

amine	T, °C	t_0, s	Avrami model n	Avrami model k, 10^{-4} s^{-1}	Jander model:κ, 10^{-5} s^{-1}
1,3-diamino-propane	200	330	0.75(3)	12.7(9)	15.0(2.7)
	180	210	0.46(2)	7.6(7)	8.0(1.2)
	160	450	0.60(3)	10.5(1.1)	41.1(3.2)
	140	480	0.76(2)	17.0(9)	13.3(1.2)
1,4-diamino-butane	200	240	0.52(4)	5.3(2.5)	7.6(90)
	180	270	0.42(2)	4.1(9)	5.6(9)
	160	270	0.51(2)	8.8(8)	2.4(6)
	140	450	0.50(4)	13.4(1.9)	4.5(7)

[a] Kinetic curves derived from study of the (112) Bragg reflection were studied (except in the 180 °C case where a detector angle of 1.16° was used and the (020) peak monitored). The induction time, t_0, was determined by inspection; the time taken for the Bragg reflection to appear above background noise. n is the Avrami coefficient; and k and κ are rate constants for the crystallization.

(40) Klug, H. P.; Alexander, L. E. *Diffraction Procedures for Polycrystalline and Amorphous Materials*, 2nd ed.; Wiley-Interscience: New York, 1974.

(41) Sharp, J. D.; Hancock, J. H. *J. Am. Ceram. Soc.* **1972**, *55*, 74.

Table 3. Results of Sharp−Hancock Analysis of Kinetic Data Describing the Crystallizations of Gallium ULM-4 Using a Variety of Gel Constituents at 180 °C[a]

amine	P source	induction time, s	Avrami model		Jander model:
			n	k, 10^{-4} s^{-1}	κ, 10^{-5}s^{-1}
1,3-diamino-propane	H_3PO_4	660	0.60(2)	36.1(2.8)	22.9(2.3)
1,3-diamino-propane	P_2O_5	780	0.61(3)	6.3(5)	46.8(3.2)
methylamine	H_3PO_4	360	0.76(3)	44.8(2.1)	6.3(1.2)
methylamine	P_2O_5	1080	0.51(2)	25.7(1.8)	11.8(2.1)

[a] Kinetic curves derived from study of the area of the (110) peak were used. Legend is as for Table 2.

reaction temperature is lowered, but generally similar values are produced so it is difficult to establish whether this effect is real.

The same approach to data analysis was performed on data collected from gallium ULM-4 syntheses, and the results are shown in Table 3. In this case two different amines were used and the effect of phosphorus source investigated (the effect of phosphorus source on the ULM-3 crystallizations will be discussed separately below). Once again Avrami exponents of less than 1 and close to 0.5 were always observed, and linear Sharp−Hancock plots were produced for a large extent of α, implying a consistent mechanism for the whole crystallization. The growth of ULM-4 appears to be more rapid than for ULM-3, since in general larger rate constants are observed, but it is difficult to draw any conclusion from this observation, particularly as the rate constants proved difficult to reproduce, even after repeated experimental runs. When methylamine is used to prepare gallium ULM-4, the induction time is significantly larger when orthophosphoric is replaced by P_2O_5. A possible explanation is that a hydrolysis step must be involved before P_2O_5 is converted into a soluble form and nucleation sites for crystallization can form.

Sharp−Hancock analysis strongly suggests that the hydrothermal crystallizations of gallium ULM-3 and ULM-4 oxyfluorophosphates are diffusion-controlled. To investigate this possibility further, a second reaction mechanism devised by Jander was tested.[39,42] Jander established for a system where chemical reaction at a phase boundary is much faster than the transport processes producing the reactive site and that three-dimensional crystal growth occurs from nucleation sites, the largest part of the growth curve can be expressed as

$$[1-(1-\alpha)^{1/3}]^2 = \kappa(t-t_0) \qquad (4)$$

The rate constant is designated κ to distinguish it from the Avrami−Eroféev rate constant used above. Clearly if this expression holds, then a plot of $(1-(1-\alpha)^{1/3})^2$ vs $(t-t_0)$ will be linear with a gradient κ. Figure 6 shows plots for the data presented above, and indeed linear graphs are observed with intercepts close to zero, as expected. For both ULM-3 and ULM-4 crystallizations studied under a variety of conditions, linear plots over a large extent of data were always obtained, and the rate constants determined from the gradients of these graphs are given in Tables 2 and 3. In some cases deviations from linearity were observed at low α, but

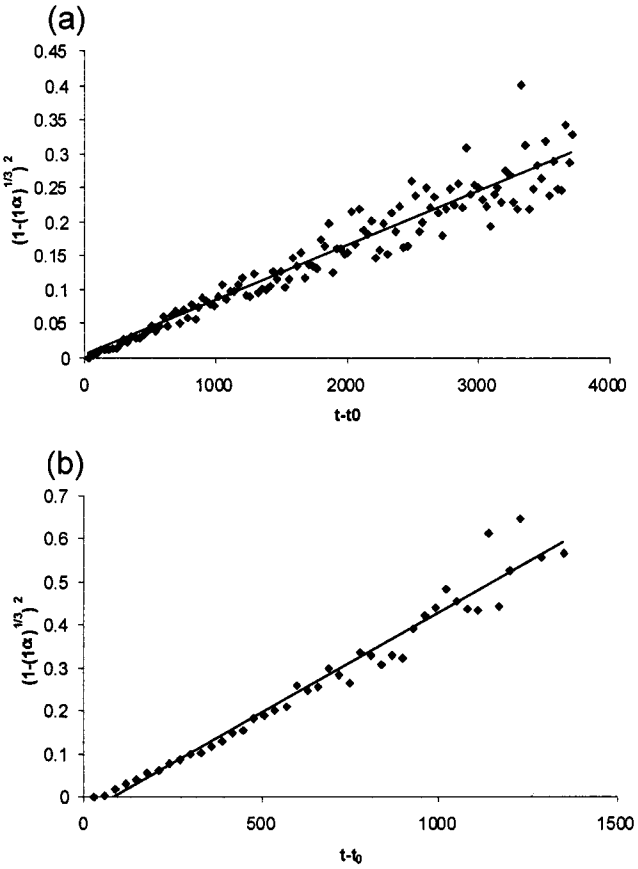

Figure 6. Plots of $(1-(1-\alpha)^{1/3})^2$ vs $(t-t_0)$, as a test of the Jander diffusion-controlled mechanism for (a) gallium ULM-3 prepared using 1,3-diaminopropane and orthophosphoric acid at 180 °C using the growth curve derived from the (111) Bragg reflection and (b) gallium ULM-4 prepared using methylamine and orthophosphoric acid at 180 °C using the growth curve derived from the (112) Bragg reflection.

this might be expected when one simple kinetic model is used to model a complete crystallization since it is highly probable that at different stages of reaction different kinetic expressions might apply. As with the Avrami−Eroféev model, there is little dependence of the rate constant of crystallization upon temperature, consistent with the diffusion-controlled reaction mechanism.

Gallium ULM-3 Phosphates Prepared Using P_2O_5. The hydrothermal synthesis of ULM-3 preparation was repeated using 1,3-diaminopropane with P_2O_5 replacing H_3PO_4 and using a temperature of 180 °C. Figure 7 shows a three-dimensional plot of the in situ EDXRD data obtained, using a detector set at 2.05° and 30 s data acquisition times, as above. The first crystalline product to appear, after only 5 min, has a strong Bragg reflections centered at 39.40, 42.77, and 61.93 keV, corresponding to d spacings of 8.68, 7.99, and 5.52 Å respectively. The positions of Bragg reflections of this phase do not match those of any compound that might be expected to crystallize from the gel used, such as an amine phosphate or gallium phosphate. The Bragg reflections of ULM-3 do not appear until ∼25 min, while the transient phase is still present, and grow in intensity while the intermediate decays. The integrated Bragg peak areas of the intermediate 8.68 Å reflection and the ULM-3 (112) Bragg peak are shown in Figure 8a, and it can be seen how the growth curve of ULM-3

(42) Jander, W. *Z. Anorg. Allg. Chem.* **1927**, *163*, 1.

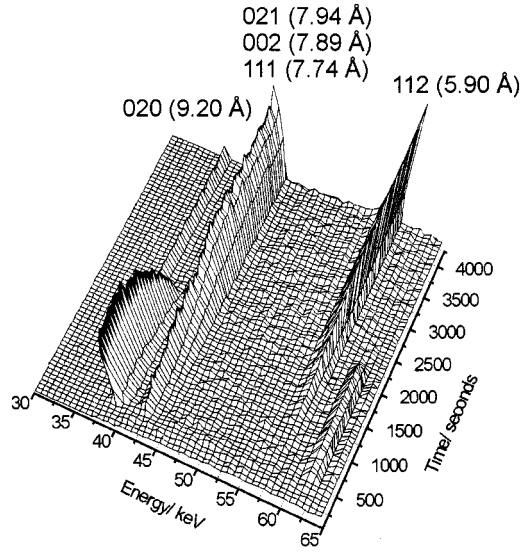

Figure 7. A three-dimensional plot of diffraction data measured during the crystallization of gallium ULM-3 when P_2O_5 is used as the phosphorus source at 180 °C.

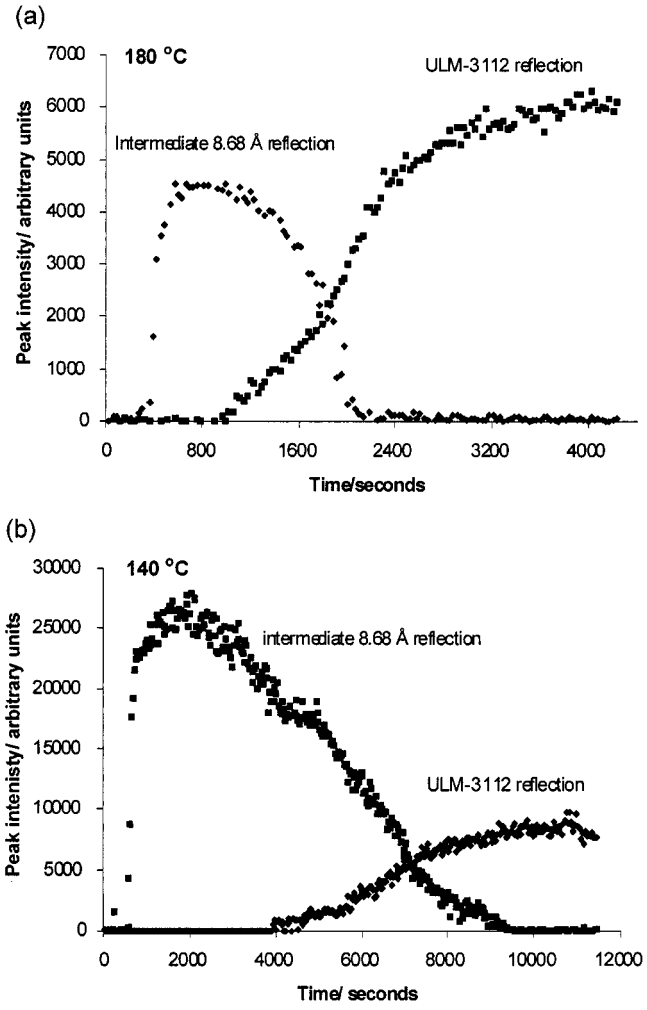

Figure 8. Results of Bragg peak area determination for the crystallization of gallium ULM-3 using P_2O_5 at (a) 180 °C and (b) 140 °C.

is affected by the growth and decay of the transient phase, having a distinctively different shape than when the compound crystallized directly from the starting mixture. The reaction was repeated at 140 °C, and identical behavior was observed, except that the intermediate phase was present for a considerably longer period of time; Figure 8b shows the integrated peak intensity for this case. A striking feature of these data is that the intensity of the intermediate reflection at the lower temperature reaches ~6 times the magnitude of its value at 180 °C (each reaction was performed with identical quantities of starting material and the intensity of the ULM-3 peak at the end of reaction shows that the same amount of product is produced in each case). Once again, after the amount of intermediate phase has passed through its maximum, the rate of product growth increases, giving rise to a distinctive kink in the growth curve of ULM-3. It also appears here that the decay of the intermediate phase is affected by the growth of the ULM-3, since at 4000 s when the ULM-3 crystallization begins, there is a small plateau in the intermediate decay curve. The data obtained at the lower temperature clearly show that a large amount of the intermediate phase decays before a substantial amount of the product has formed; the curves describing decay of intermediate and growth of product clearly do not cross at 50%. This suggests that the transformation of the intermediate phase to ULM-3 must involve either dissolution of the intermediate, or transformation via an amorphous phase.

With the aim of gaining more information about the nature of the intermediate phase observed in the in situ experiments, quenching experiments were performed to isolate the new compound for further characterization. Using the in situ apparatus, the gallium ULM-3 reaction mixture was heated at 140 °C until the intensity of the intermediate Bragg reflections was significant (~15 min), and before the ULM-3 Bragg reflections were observed. At this point the hydrothermal cell was removed from the heating block and rapidly cooled to room temperature by plunging into cold water. The solid was recovered from the cooled mixture by filtration and washed with distilled water and acetone. An X-ray powder diffraction pattern recorded using a Philips PW1729 X-ray diffractometer (Cu Kα radiation) is shown in Figure 9. Although the strong Bragg reflections of this phase do not match those seen in situ, a crystalline material with different strong low-angle Bragg reflections than ULM-3 is present. Repeated quenching experiments using the in situ apparatus and in the laboratory using Parr autoclaves were performed and it proved impossible to isolate the intermediate compound; in every case either unreacted starting material or the second crystalline phase was recovered. It is therefore likely that the phase seen in situ is either unstable under ambient conditions, or converts to the second phase during recovery (filtering and washing) from the reaction mixture. A crystalline phase whose powder pattern matches very closely that of the material isolated was subsequently prepared in a more crystalline form and containing fewer impurity peaks, by standing a gallium phosphate gel of composition Ga_2O_3:2 P_2O_5:1.9 1,3-diaminopropane:2.0 HF:70 H_2O (i.e., the same as the gel used to prepare ULM-3 but with double the quantity of P_2O_5) at room temperature for 1 month; its X-ray powder pattern is shown in Figure 9. Excluding strong Bragg reflections of the contaminant gallium oxide phase, the powder diffraction pattern could be

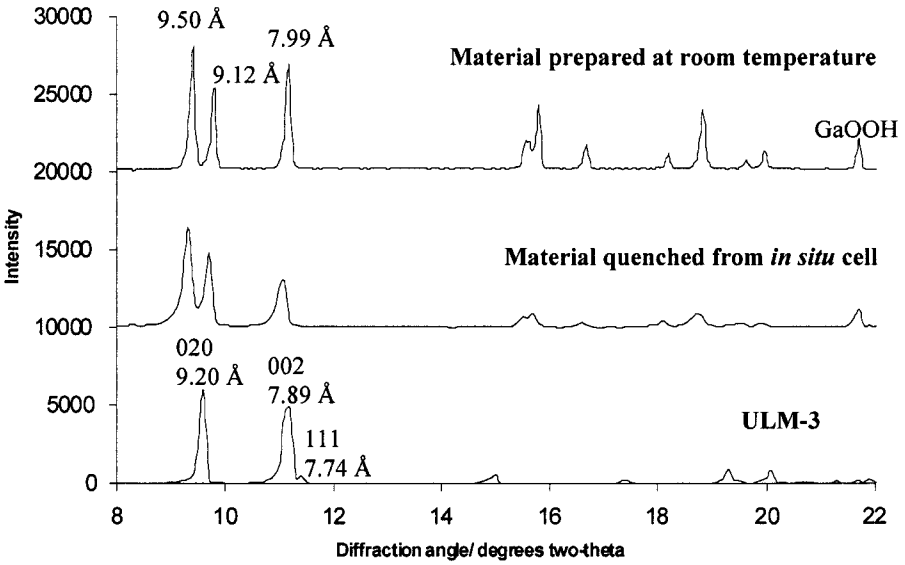

Figure 9. Laboratory powder X-ray diffraction patterns of ULM-3, material recovered from the in situ cell after quenching the ULM-3 (P_2O_5) reaction after 15 min at 140 °C, and (c) material prepared after standing the ULM-3 gel ($2P_2O_5$) for 1 month at room temperature. The *d* spacings of strong reflections are indicated.

successfully indexed using 20 strong reflections and the auto indexing program TREOR90[43] with a monoclinic cell (a = 9.94024 Å, b = 7.15773 Å, c= 9.53648 Å; β = 108.80°). No match to this cell could be found among known gallium and aluminum phosphate phases. Analytical electron microscopy of the material quenched recovered from the in situ experiment and the material prepared at room temperature showed that in both cases the majority of crystallites contained all of the elements Ga, P, O, F, C, and N and that the Ga:P ratio was 1:2. Each material contained small amounts of crystallites containing only Ga and O, presumably the unreacted gallium source.

Discussion

The observation of diffusion-controlled kinetics in the synthesis of open-framework gallium oxyfluorophosphates with the ULM-3 and ULM-4 structures is entirely consistent with our previous studies of the hydrothermal crystallization of the large-pore gallium oxyfluorophosphate ULM-5.[27,28] In situ study of phosphate crystallizations has not been performed extensively, and there is only a small amount of kinetic data available in the literature for comparison, but the crystallization kinetics of the ULM-*n* compounds differ considerably from data that are available. For example, Norby and Christensen in their in situ study of the crystallization of MeALPOs found that the Avrami coefficient is always greater than 1, and in some cases as high as 10, indicating mechanisms in which nucleation continues after crystallization has begun, and thus crystal growth is affected by the continuing formation of nucleation sites.[9,10] It must be borne in mind that most previous in situ studies used angular dispersive X-ray difraction which requires very small sample volumes (usually contained in ~0.5 mm diameter capillaries) and thus results may not be directly comparable to ours in which genuine laboratory conditions are employed. The use of hydrofluoric acid in the synthesis of the ULM-*n* compounds is a possible explanation for the difference in kinetics observed for the hydrothermal synthesis of other phosphates. It is most likely that hydrofluoric acid has a mineralizing effect, allowing rapid assimilation of other reagents into a soluble, highly reactive form. Thus the rate-determining step of reaction is only the dissolution of reagents and the formation of a homogeneous reaction mixture; crystallization can then occur instantaneously. The stirring used in our in situ experiment could possibly enhance the mixing process, but it is unlikely that it changes the course of reaction. Clearly in situ diffraction methods do not hold the key to a full understanding of the crystallizations, when the process occurring in solution determine the rate of reaction. Other information must be sought in which the changes occurring in solution are studied and related to the crystallization process. Our experiments have provided a firm foundation on which to base a reaction mechanism. We hope to probe changes occurring in solution and relate them to the crystallization data we have by using techniques such as NMR spectroscopy and EXAFS. This a current area of our research and an area which still requires development of new methodology if in situ studies are to be performed.

The observation of transient intermediate phases during the preparation of the ULM-*n* compounds when certain combinations of reagents are used in the initial reaction mixture remains unique among the phosphates so far studied using in situ diffraction methods. The use of P_2O_5 instead of phosphoric acid must be important in understanding the formation of these previously unknown phases since both gallium ULM-3 and gallium ULM-5 may form via intermediates when P_2O_5 is used. The growth and decay of the intermediate phases has a marked effect on the crystallization curve of the product. Interestingly Christensen et al. in their study of the crystallization of ZnAlPO-47 observed a similarly shaped product growth curve and suggested that this is indicative of the presence of an intermediate transient

(43) TREOR90, Werner, P. E. University of Stockholm, Sweden, 1990.

phase, although in their case assumed to be an amorphous material, since no Bragg reflections other than the product were observed.[8] Clearly mathematical modeling of the kinetics and mechanism of the conversion of the intermediate phase in to ULM-3 will be an extremely complex process and structural characterization of the intermediate phase will be vital in order to make progress with this. The transient phases we observe in situ are most probably unstable under ambient conditions, since quenching experiments have not led to their successful isolation. However, the crystalline gallium phosphate we have isolated and that can be prepared at room temperature is likely to be structurally related to the intermediate phase. Recently Oliver et al. showed that alkylammonium phosphates may crystallize at room temperature from aluminophosphate gels, usually heated under hydrothermal conditions, and suggested that such materials could commonly crystallize from phosphate gels and be mistakenly assigned as new metal phosphates.[44] Here we observe very different behavior, since electron microscopy conclusively shows that a gallium phosphate is formed at room temperature. If the intermediate phase has the same Ga:P ratio of 1:2, then there cannot be a direct solid-state transformation in its conversion to ULM-3, since ULM-3 contains Ga and P in the ratio 1:1. This is consistent with the observation that the growth curve of ULM-3 does not intersect with the decay curve of the intermediate at 50%, suggesting some dissolution is taking place. It is interesting to note that the open-framework phosphates of aluminum and gallium so far reported in the literature with a metal:phosphorus ratio of 1:2 all adopt layered[45,46] or chain[47−49] structures. Although it does not necessarily follow that the new phases we observe here are low-dimensional, the possibility that they might be is compelling.

Our in situ study has highlighted the complexity of the Ga_2O_3:P_2O_5:HF:H_2O:1,3-diaminopropane system and suggests that although ULM-3 and ULM-4 are stable materials formed under hydrothermal heating, other gallium phosphates exist in the system, including phases that may be prepared under more moderate conditions. Clearly the precise composition and pH of the gel is very important in deciding which course of reaction is taken and whether an intermediate phase is observed. Given the structural similarity between ULM-3 and ULM-4, it is noteworthy that no intermediates phases are observed during the ULM-4 crystallizations when P_2O_5 is used as the phosphorus source; the difference in gel pH must have an important role to play in this system. Structural characterization of the new phases we have identified here, as the result of in situ studies, will be of the utmost importance in a greater understanding of the kinetics of these reactions.

Acknowledgment. We thank the Leverhulme Trust, the British Council (Alliance project) and the Novartis Fellowship Trust for financial support. The EPSRC is acknowledged for financial support and for provision of facilities at Daresbury Laboratory. We thank Dr. S. M. Clark (Daresbury) for assistance with running the EDXRD experiments.

Supporting Information Available: Plots of kinetic data for all reactions studied. This material is available free of charge via the Internet at http://pubs.acs.org.

CM990271C

(44) Oliver, S. R.; Lough, A. J.; Ozin, G. A. *Inorg. Chem.* **1998**, *37*, 5021.
(45) Bircsak, Z.; Harrison, W. T. A. *Chem. Mater.* **1998**, *10*, 3016.
(46) Jones, R. H.; Thomas, J. M.; Xu, R.; Xu, Y.; Cheetham, A. K.; Bieber, D. *J. Chem. Soc., Chem. Commun.* **1990**, 1170.
(47) Chippindale, A. M.; Turner, C. *J. Solid State Chem.* **1997**, *128*, 318.
(48) Chippindale, A. M.; Bond, A. D.; Law, A. D.; Cowley, A. R. *J. Solid State Chem.* **1998**, *136*, 227.
(49) Jasper, J. D.; Wilkinson, A. P. *Chem. Mater.* **1998**, *10*, 1664.